PNAS

Supporting Information for

Audible enclaves crafted by nonlinear self-bending ultrasonic beams

Jia-Xin Zhong, Jun Ji, Xiaoxing Xia, Hyeonu Heo, Yun Jing

Corresponding Author:
Yun Jing
E-mail: yqj5201@psu.edu

This PDF file includes:

Figs. S1 to S17
Legend for Movie S1

Other supporting materials for this manuscript include the following:

Movie S1

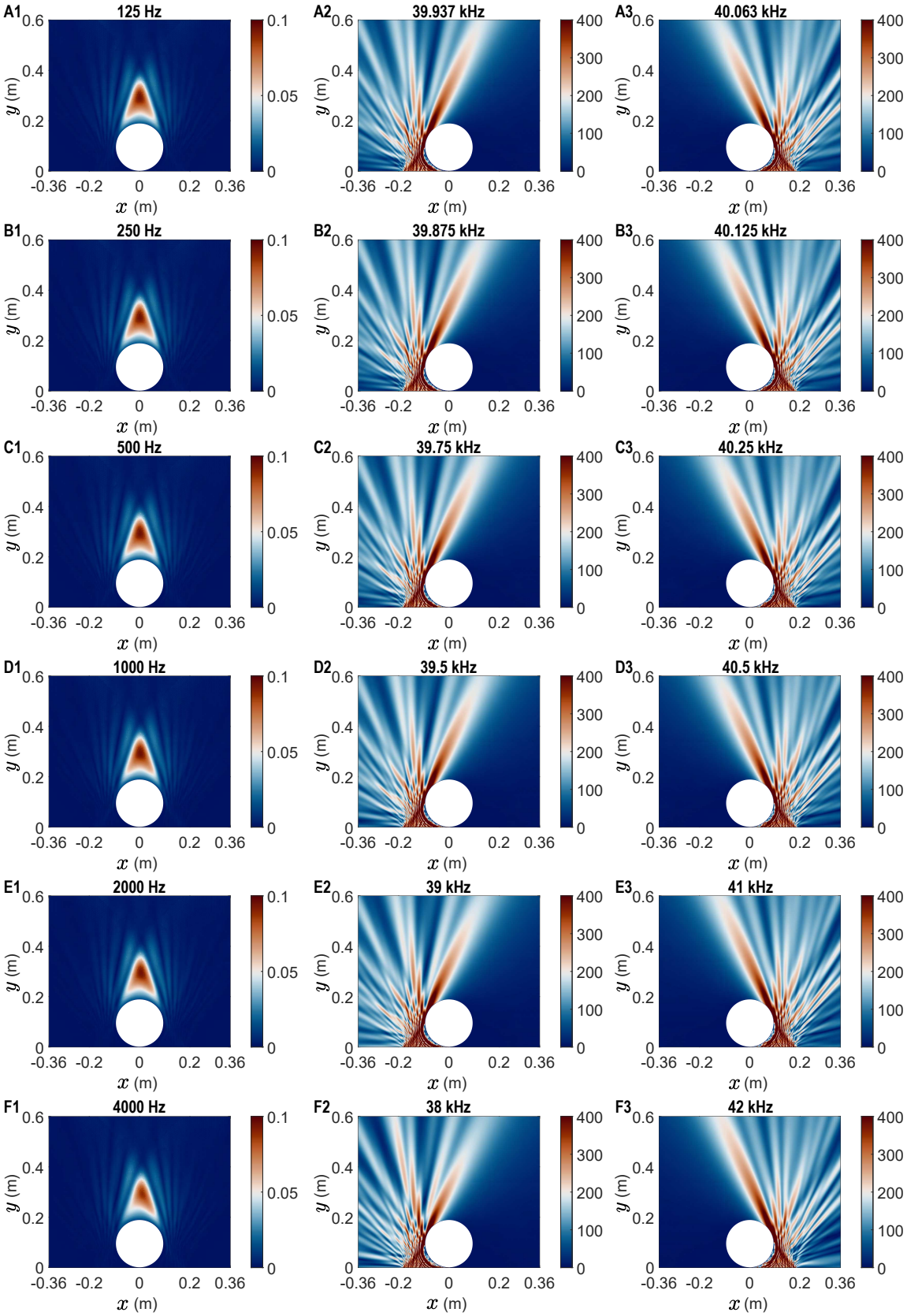

Fig. S1. Simulated sound field distributions (in pascals, Pa) in the presence of a circular acoustically hard obstacle with a radius of 90 mm. Audio sound fields at (A1) 125 Hz, (B1) 250 Hz, (C1) 500 Hz, (D1) 1 kHz, (E1) 2 kHz, and (F1) 4 kHz. Columns (2) and (3) represent the corresponding ultrasound fields. Audible enclaves centered at $(x, y) = (0, 325\,\text{mm})$ can be observed in column (1).

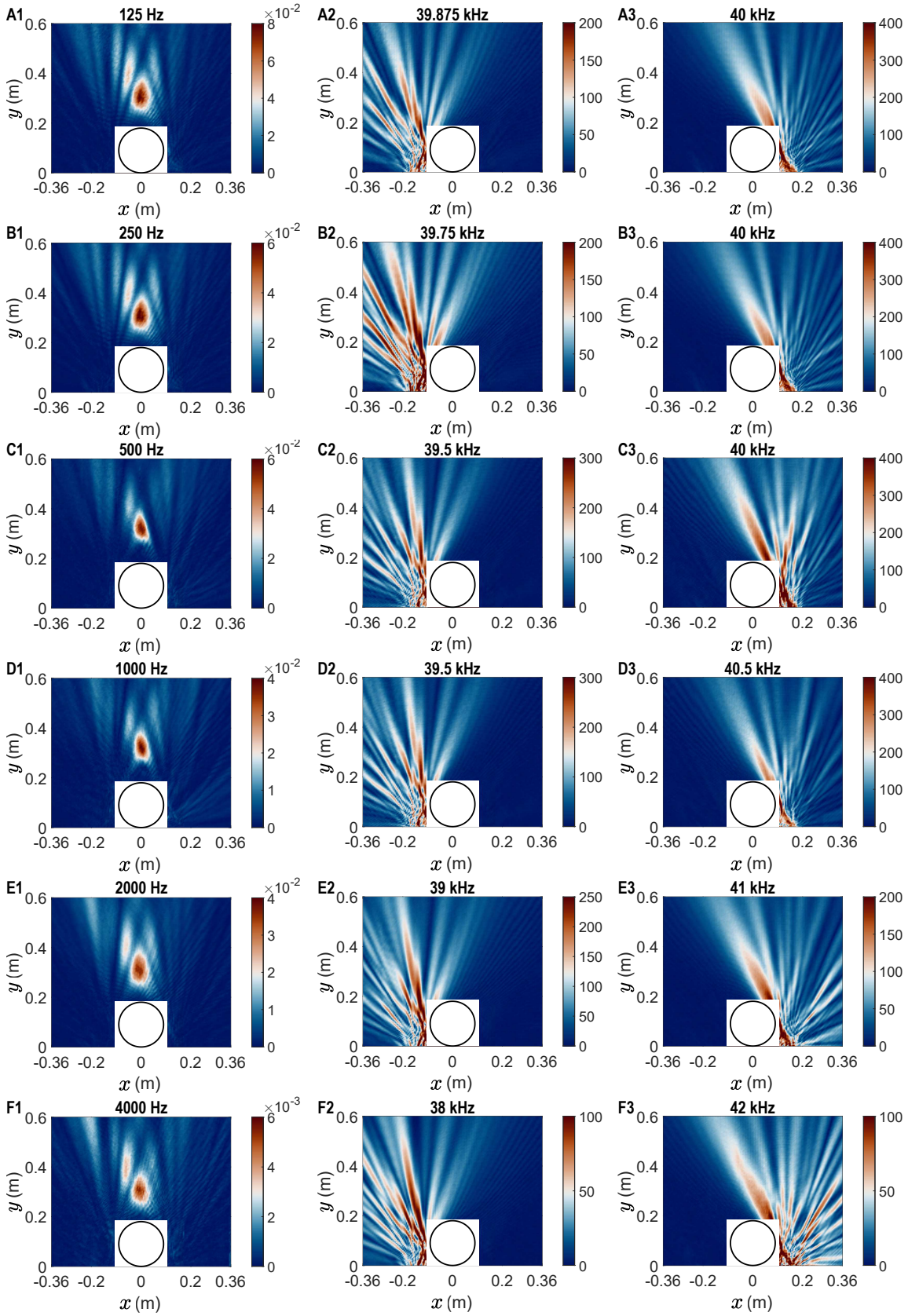

Fig. S2. Measured sound field distributions (in pascals, Pa) in the presence of a circular acoustically hard obstacle with a radius of 90 mm. Audio sound fields at (A1) 125 Hz, (B1) 250 Hz, (C1) 500 Hz, (D1) 1 kHz, (E1) 2 kHz, and (F1) 4 kHz. Columns (2) and (3) represent the associated ultrasound fields. In all cases, same metasurfaces are utilized. Audible enclaves centered at $(x, y) =$ (0, 325 mm) can be observed in column (1).

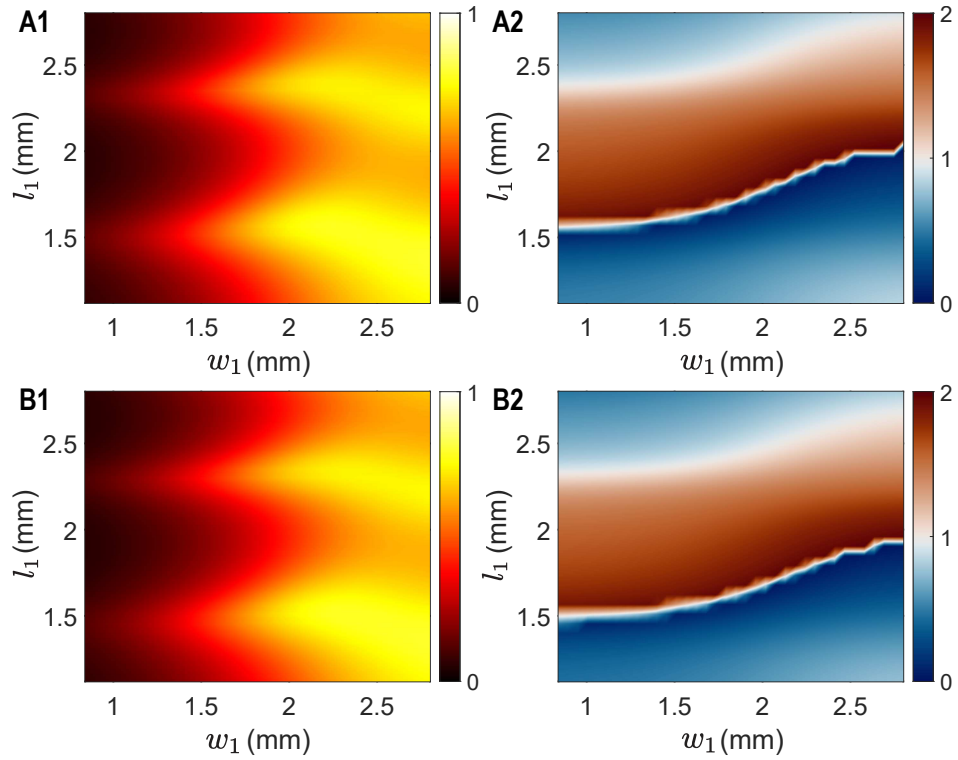

Fig. S3. (1) Amplitude and (2) phase (in π) of the transmission coefficient of the unit cell as a function of the geometric parameters w_1 and l_1 at (A) 39.5 kHz and (B) 40 kHz.

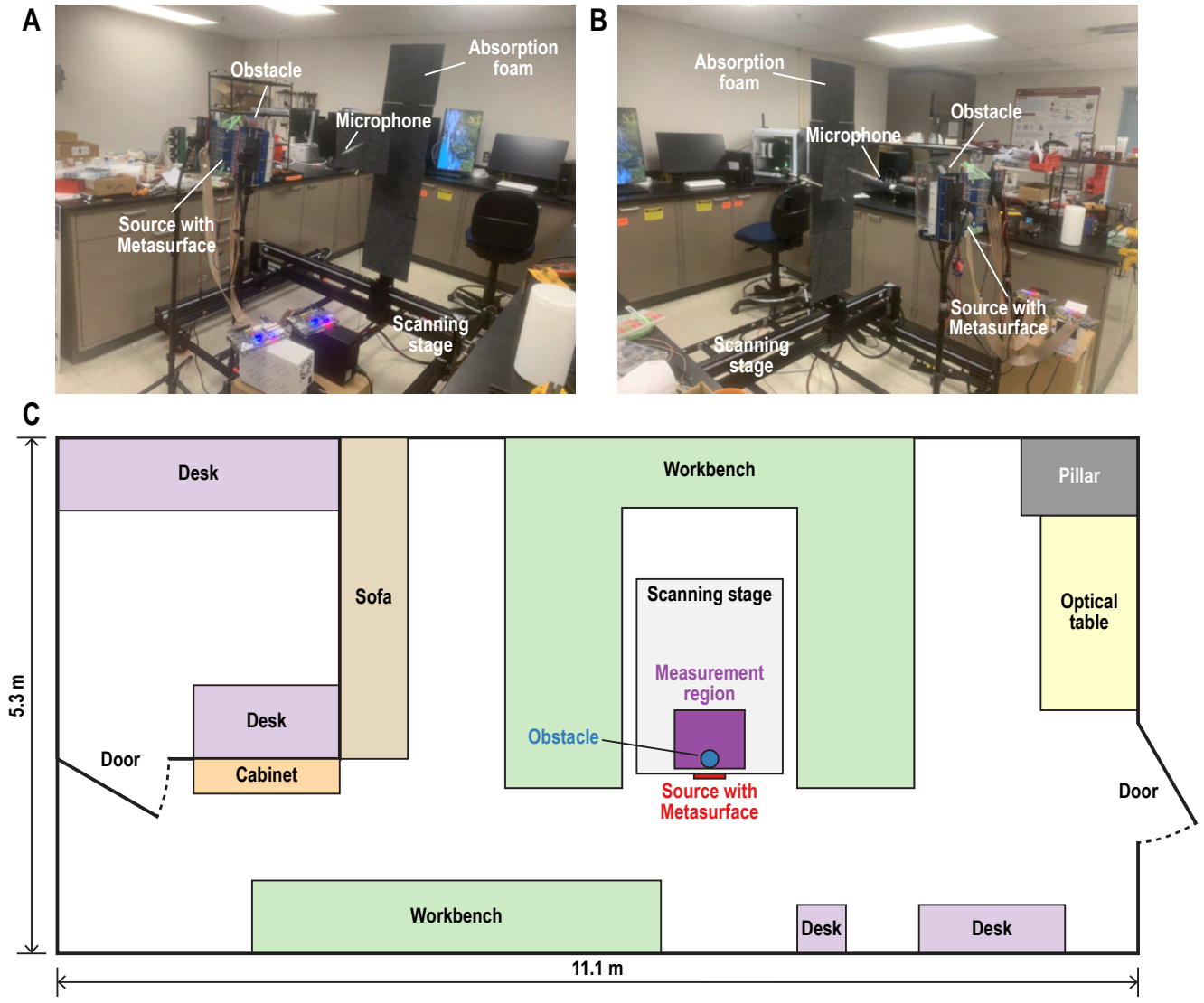

Fig. S4. (A, B) Photos and (C) schematic drawing of the laboratory where experiments were conducted. The laboratory room measures 11.1 m × 5.3 m × 2.4 m. It is furnished workbenches, desks, cabinets, optical tables, etc.

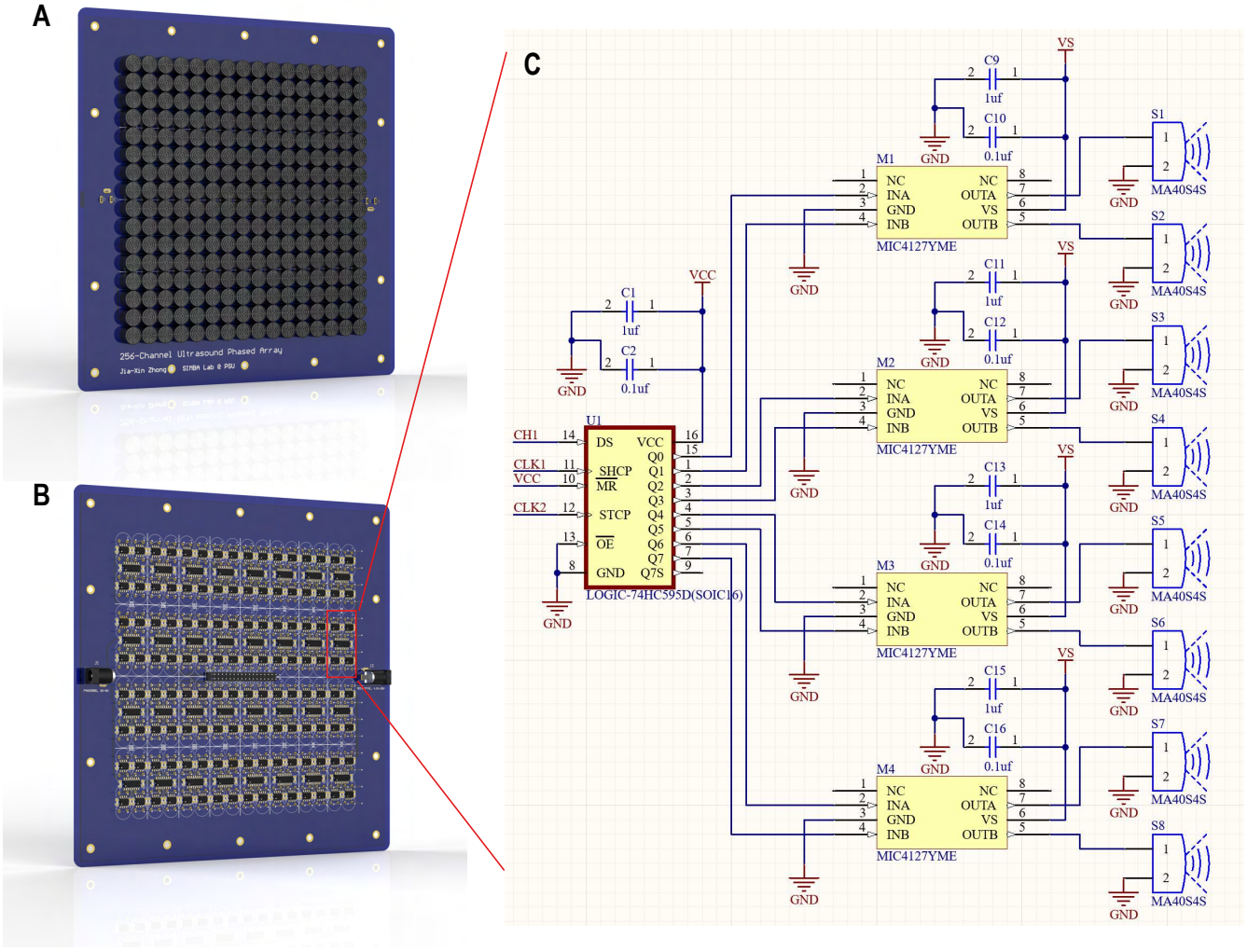

Fig. S5. Laboratory-made airborne ultrasound array used in experiments. It consists of $16 \times 16 = 256$ PZT-based ultrasound transducers (Murata, MA40S4S) with a diameter of 10 mm and a center frequency of 40 kHz. (A) Front view. (B) Back view. (C) Schematic diagram of one group of the circuit comprising 8 transducers, 4 power amplifiers, 1 shift register, and some capacitors.

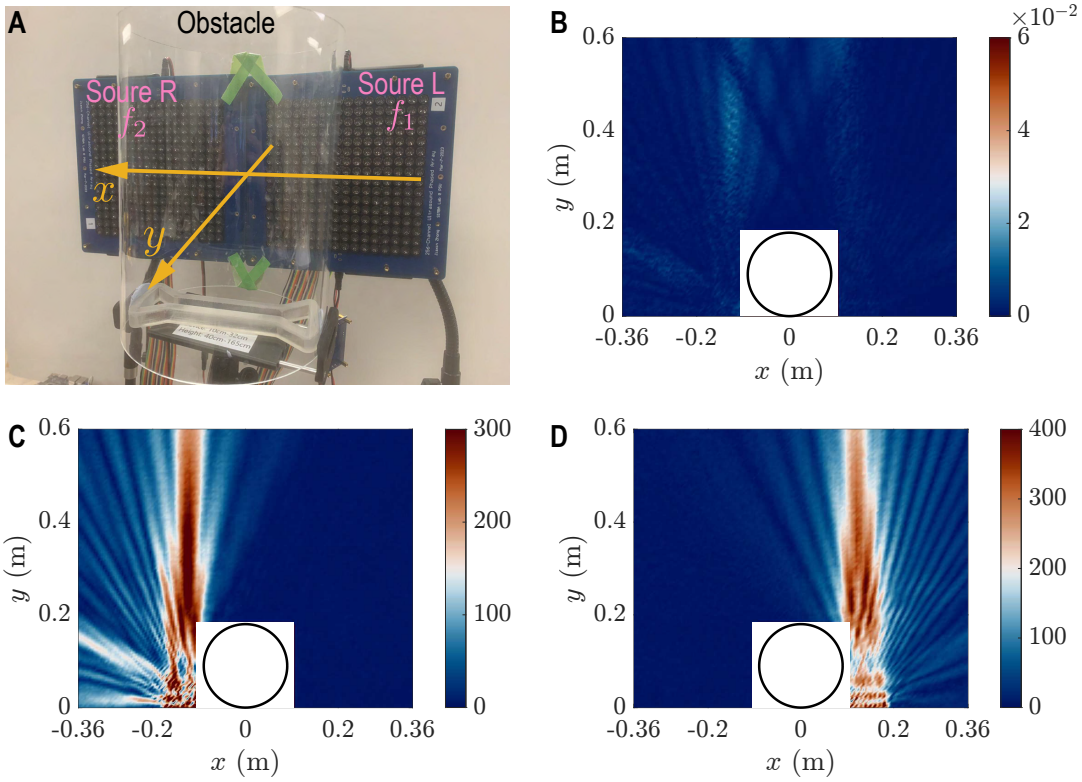

Fig. S6. Measured sound fields (in pascals, Pa) without using the metasurfaces. (A) Photo of the experimental setup, where sources L and R emit ultrasonic beams at frequencies $f_1 = 39.5\,\mathrm{kHz}$ and $f_2 = 40\,\mathrm{kHz}$, respectively. An acoustically hard circular cylinder with a radius of 90 mm is placed to obstruct the beams. Measured (B) audio sound ($f = 500\,\mathrm{Hz}$) and ultrasound (B, 39.5 kHz; C, 40 kHz) fields. In contrast to Fig. 2A in the main text, the audible enclave is not formed.

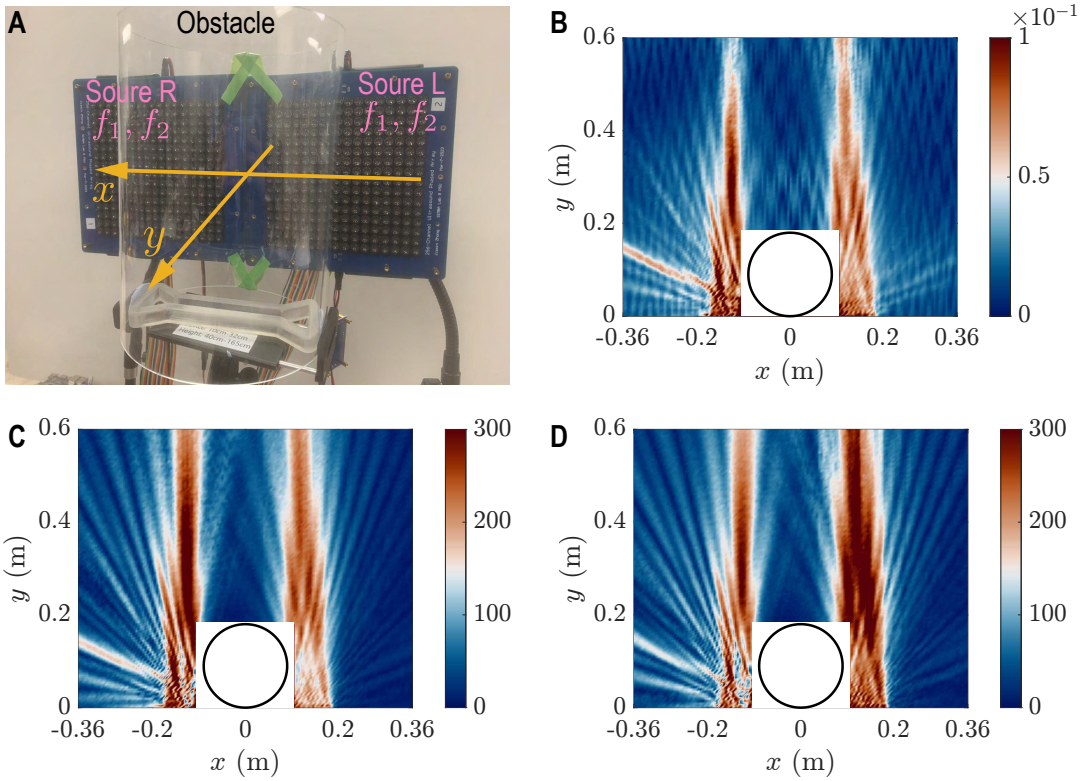

Fig. S7. Measured sound fields (in pascals, Pa) without using the metasurfaces. (A) Photo of the experimental setup, where sources L and R emit ultrasonic beams at both frequencies $f_1 = 39.5\,\mathrm{kHz}$ and $f_2 = 40\,\mathrm{kHz}$. An acoustically hard circular cylinder with a radius of 90 mm is placed to obstruct the beams. Measured (B) audio sound ($f = 500\,\mathrm{Hz}$) and ultrasound (B, 39.5 kHz; C, 40 kHz) fields. In contrast to Fig. 2A in the main text, the audible enclave is not formed. Instead, two directional audio beams are generated.

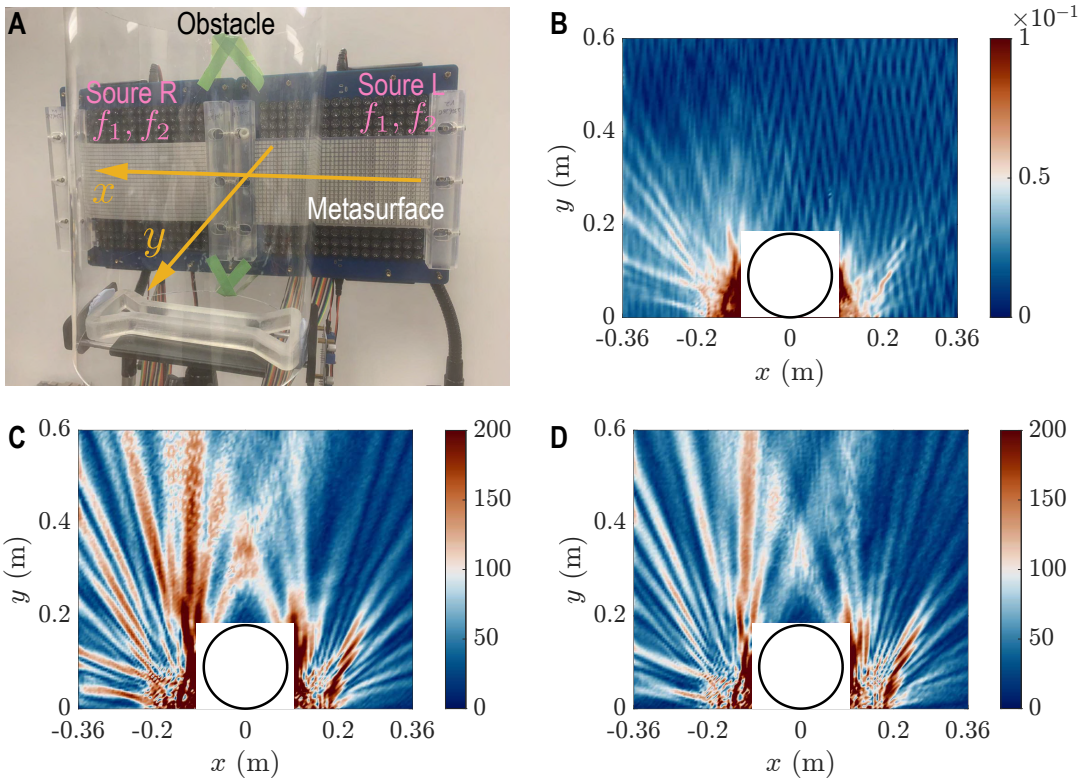

Fig. S8. Measured sound fields (in pascals, Pa) with using the metasurfaces. (A) Photo of the experimental setup, where sources L and R emit ultrasonic beams at both frequencies $f_1 = 39.5\,\mathrm{kHz}$ and $f_2 = 40\,\mathrm{kHz}$. An acoustically hard circular cylinder with a radius of 90 mm is placed to obstruct the beams. Measured (B) audio sound ($f = 500\,\mathrm{Hz}$) and ultrasound (B, 39.5 kHz; C, 40 kHz) fields. In contrast to Fig. 2A in the main text, the audible enclave is not formed behind the obstacle. Instead, significant audible signals are observed near the sources.

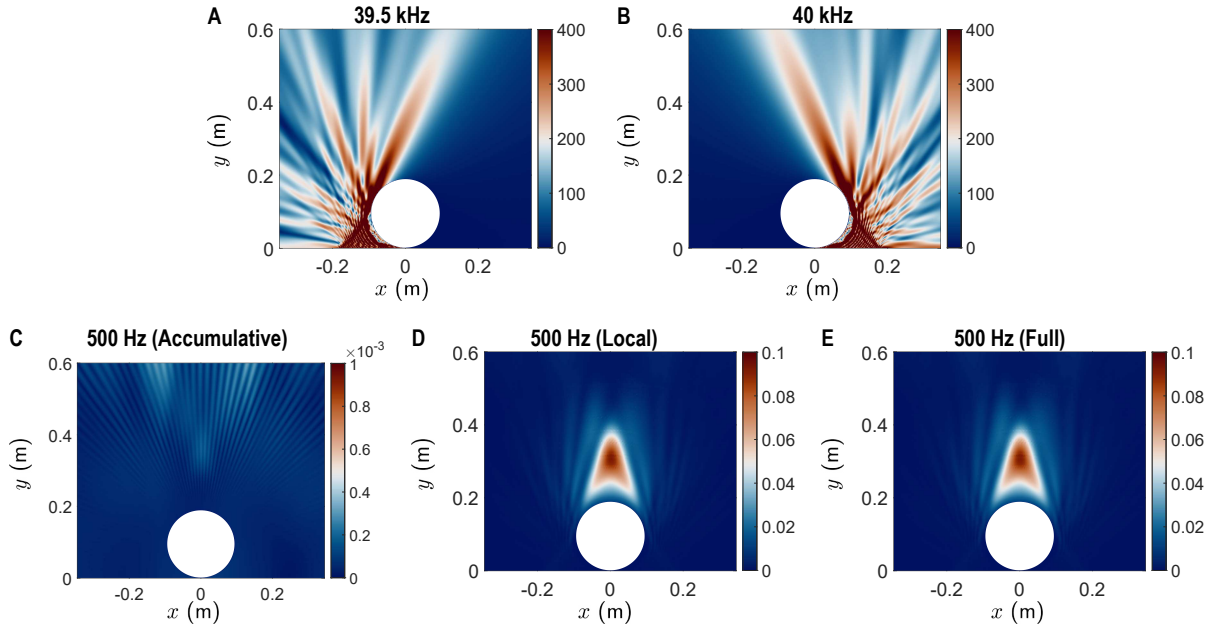

Fig. S9. Results of our proposed audible enclave. Simulated sound field distributions (Pa) for a pure-tone audio signal excitation at 500 Hz. (A, B) Self-bending ultrasonic beams at frequencies of (A) 39.5 kHz and (B) 40 kHz. (C, D, E) Corresponding audio sound fields at 500 Hz generated using (C) cumulative nonlinear effects only, (D) local nonlinear effects only, and (E) both cumulative and local nonlinear effects.

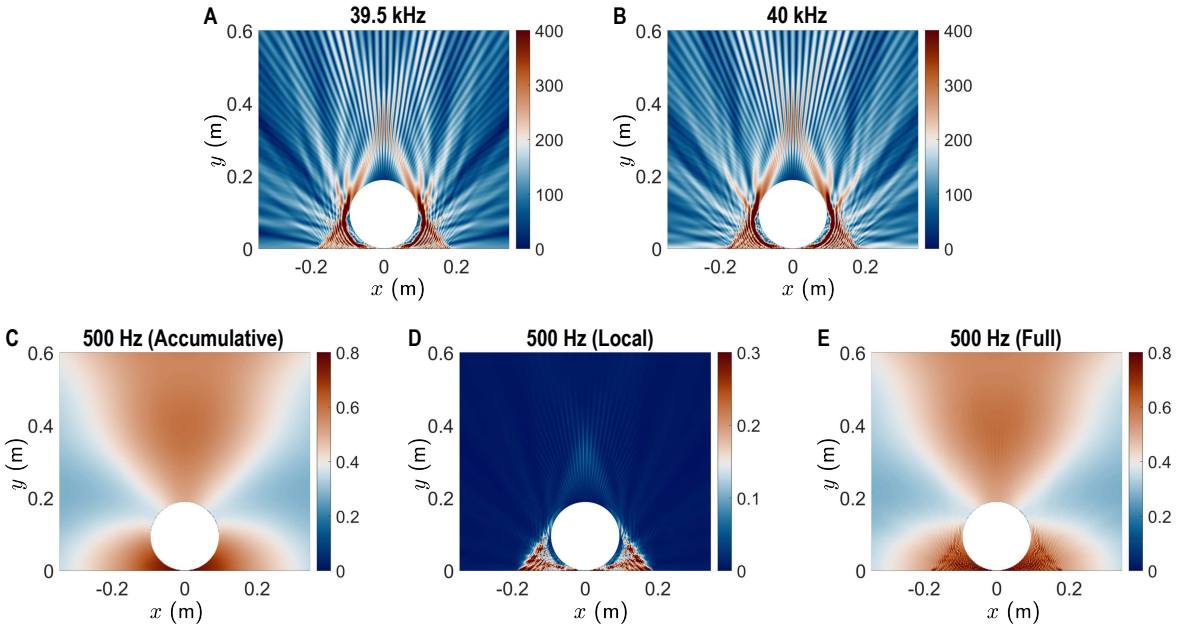

Fig. S10. Results of the parametric array. Simulated sound field distributions (Pa) for a pure-tone audio signal excitation at 500 Hz. (A, B) Self-bending ultrasonic beams at frequencies of (A) 39.5 kHz and (B) 40 kHz. (C, D, E) Corresponding audio sound fields at 500 Hz generated using (C) cumulative nonlinear effects only, (D) local nonlinear effects only, and (E) both cumulative and local nonlinear effects.

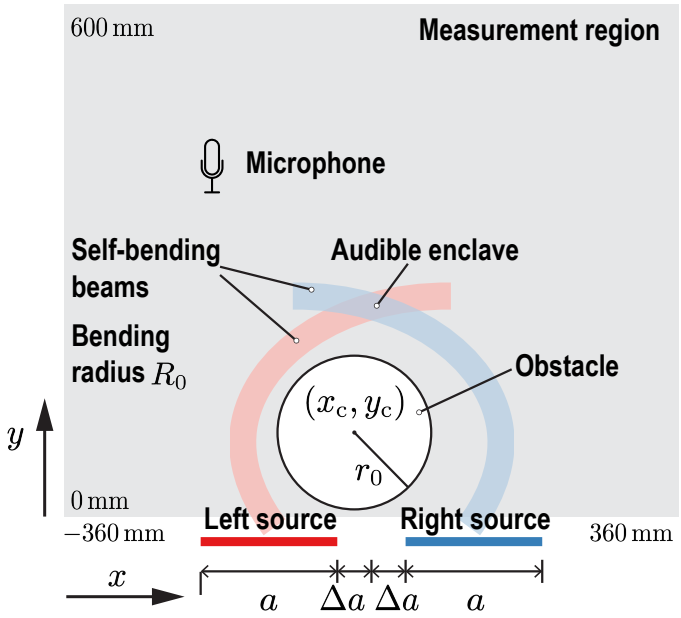

Fig. S11. Sketch of the formation of an audible enclave and parameter definitions. **Obstacle radius** r_0: Varied to examine the effects of head size. **Obstacle displacement** x_c: Adjusted to analyze the impact of head position. **Source separation** Δa: Modified as a potential solution to maintain robust audible enclave formation. **Bending radius** R_0: Optimized to improve the robustness of self-bending beams. **Source size** a: Increased to further enhance the robustness.

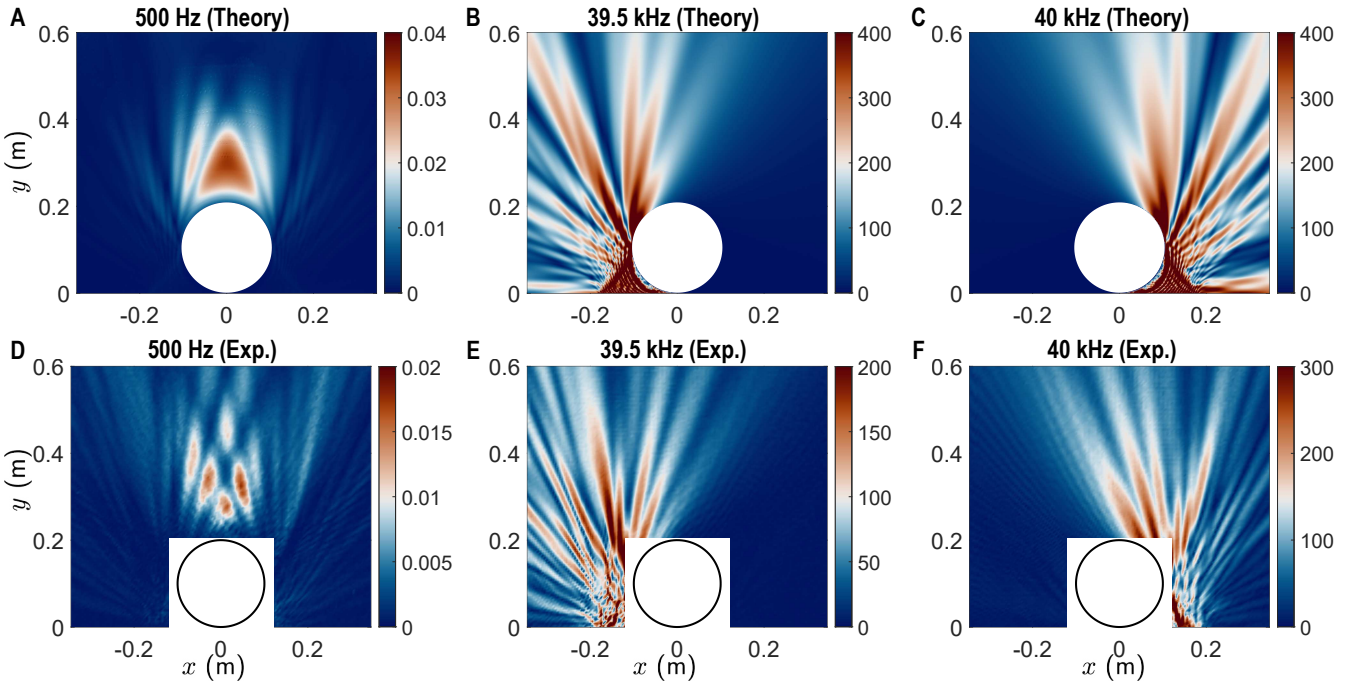

Fig. S12. (A, B, C) Simulated and (D, E, F) measured sound field distributions (Pa) with a larger obstacle radius of $r_0 = 100\,\mathrm{mm}$. Other parameters defined in Fig. S11 are: $x_\mathrm{c} = 0\,\mathrm{mm}$, $\Delta a = 25\,\mathrm{mm}$, $R_0 = 80\,\mathrm{mm}$, and $a = 16\,\mathrm{cm}$. Self-bending ultrasonic beams at (B, E) 39.5 kHz and (C, F) 40 kHz.

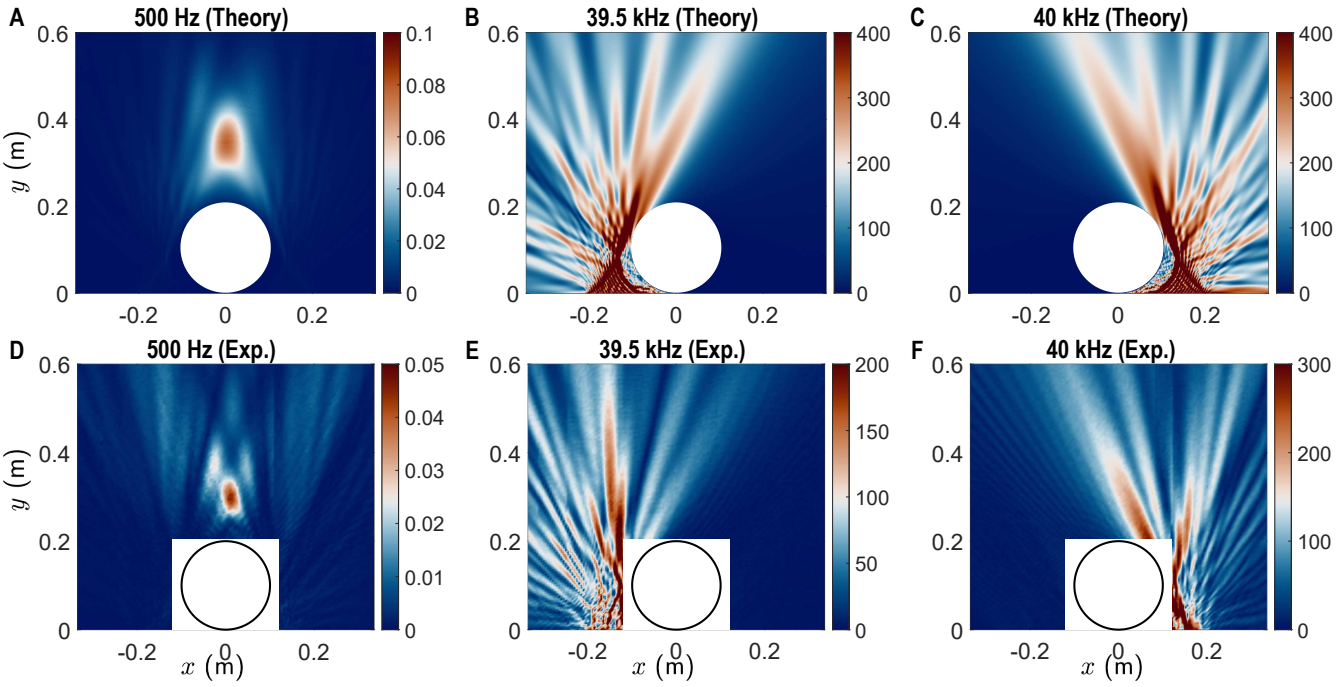

Fig. S13. (A, B, C) Simulated and (D, E, F) measured sound field distributions (Pa) with a larger obstacle radius of $r_0 = 100\,\mathrm{mm}$ and a larger source separation of $\Delta a = 50\,\mathrm{mm}$. Other parameters defined in Fig. S11 are $x_c = 0\,\mathrm{mm}$, $R_0 = 80\,\mathrm{mm}$, and $a = 16\,\mathrm{mm}$. Self-bending ultrasonic beams at (B, E) 39.5 kHz and (C, F) 40 kHz.

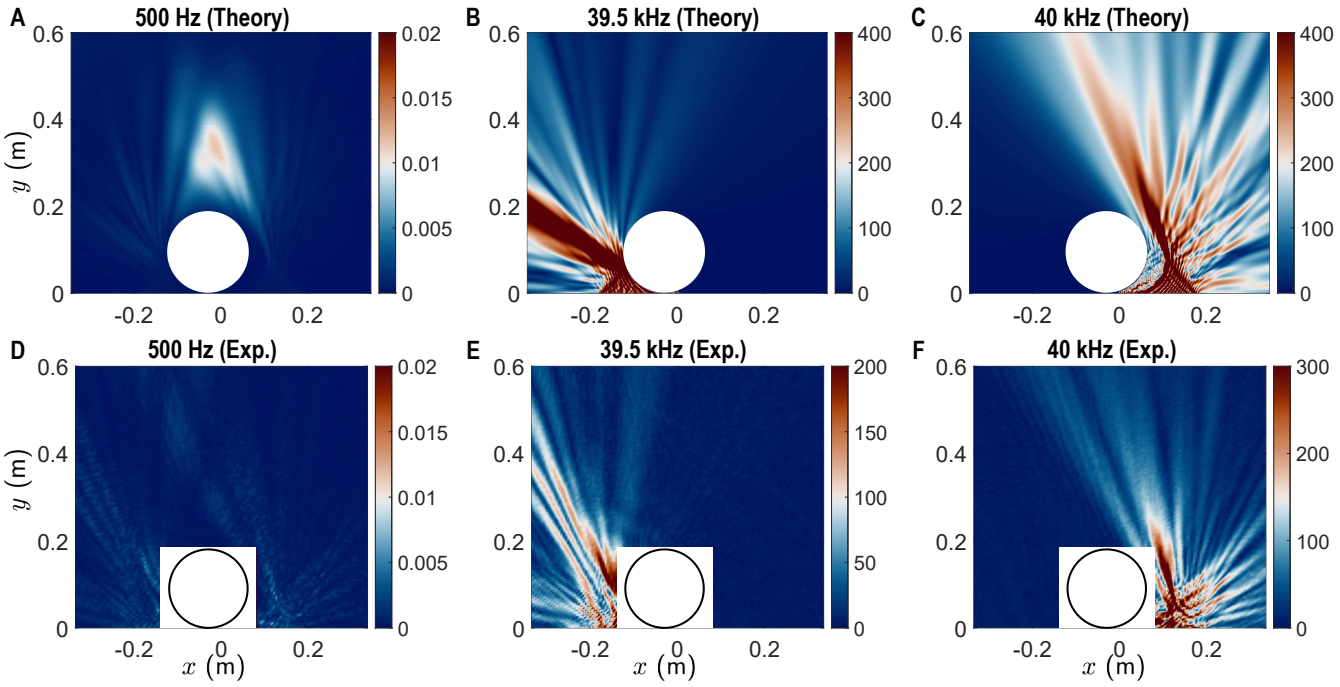

Fig. S14. (A, B, C) Simulated and (D, E, F) measured sound field distributions (Pa) with a head position of $x_{\mathrm{c}} = -30\,\mathrm{mm}$. Other parameters defined in Fig. S11 are: $r_0 = 90\,\mathrm{mm}$, $\Delta a = 50\,\mathrm{mm}$, $R_0 = 80\,\mathrm{mm}$, and $a = 16\,\mathrm{cm}$. Self-bending ultrasonic beams at (B, E) 39.5 kHz and (C, F) 40 kHz.

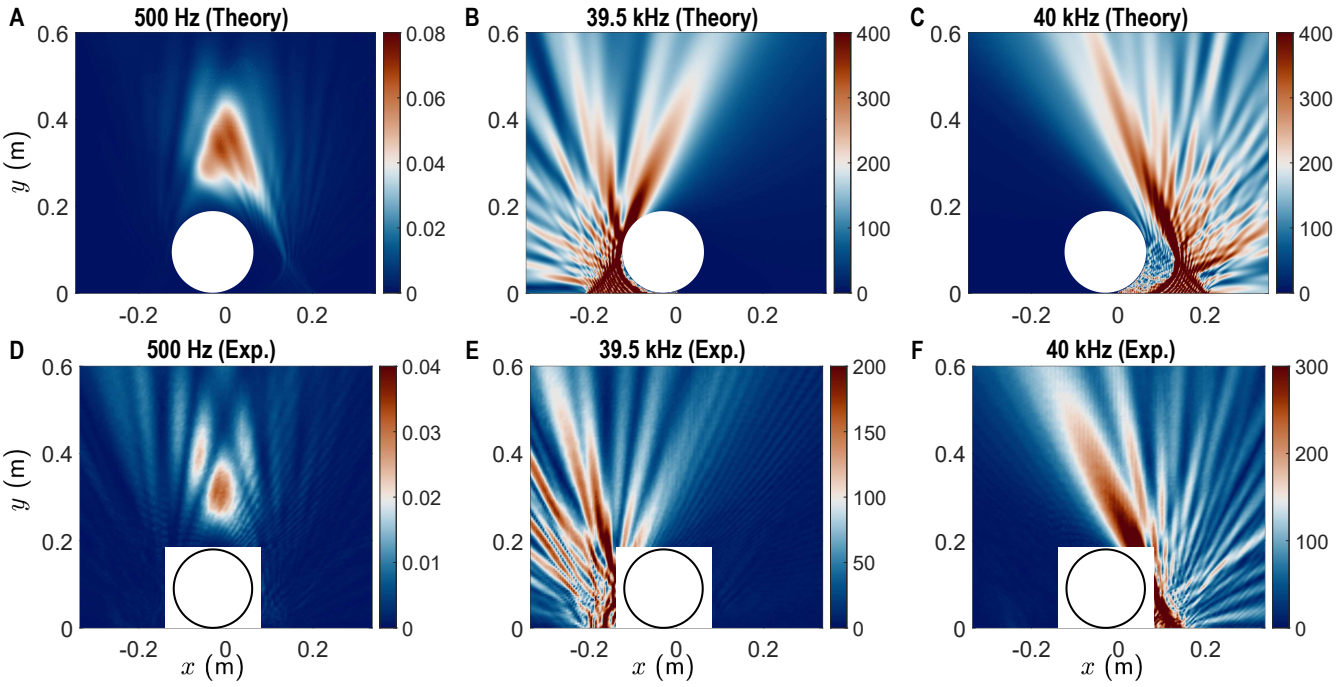

Fig. S15. (A, B, C) Simulated and (D, E, F) measured sound field distributions (Pa) with a head position of $x_c = -30\,\mathrm{mm}$ and a larger source separation of $\Delta a = 50\,\mathrm{mm}$. Other parameters defined in Fig. S11 are: $r_0 = 90\,\mathrm{mm}$, $R_0 = 80\,\mathrm{mm}$, and $a = 16\,\mathrm{cm}$. Self-bending ultrasonic beams at (B, E) 39.5 kHz and (C, F) 40 kHz.

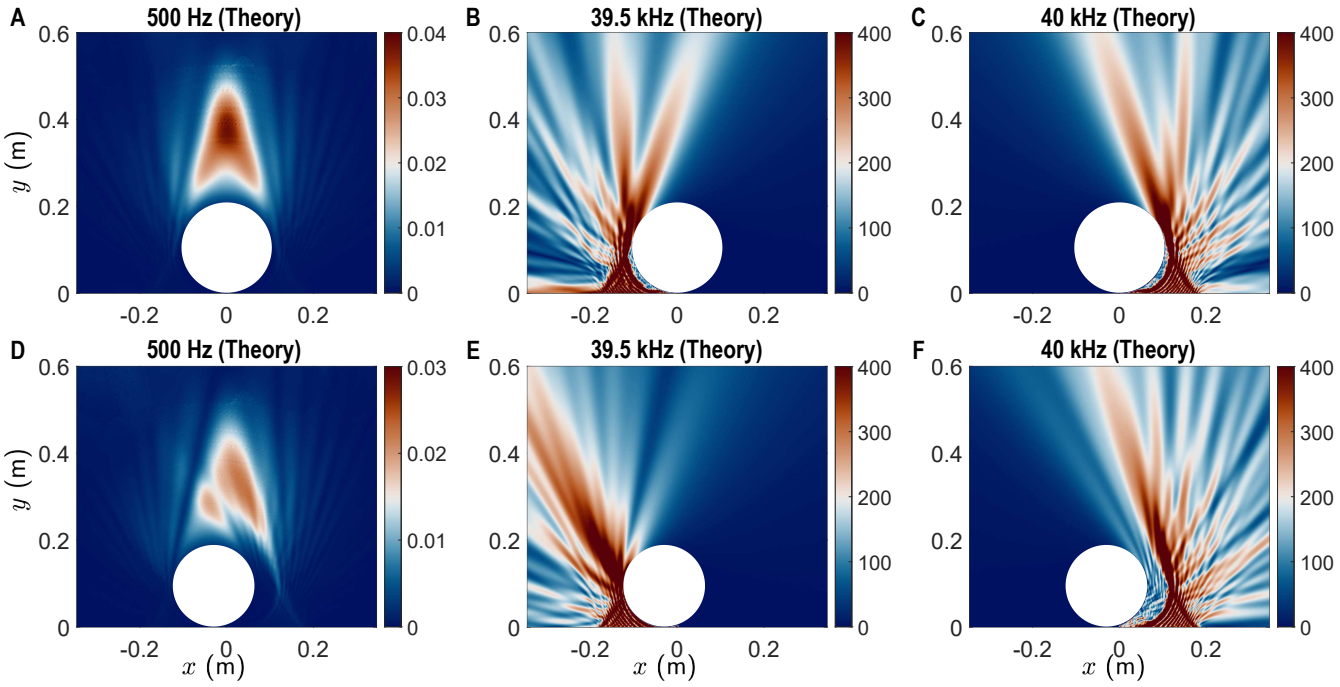

Fig. S16. Simulated sound field distributions with a larger bending radius of $R_0 = 90\,\mathrm{mm}$. Other parameters defined in Fig. S11 are: $\Delta a = 25\,\mathrm{mm}$, $a = 16\,\mathrm{cm}$, (A, B, C) $x_\mathrm{c} = 0$, $r_0 = 100\,\mathrm{mm}$, and (D, E, F) $x_\mathrm{c} = -30\,\mathrm{mm}$, $r_0 = 90\,\mathrm{mm}$. (A, D) Audio sound fields at 500 Hz. Self-bending ultrasonic beams at (B, E) 39.5 kHz and (C, F) 40 kHz.

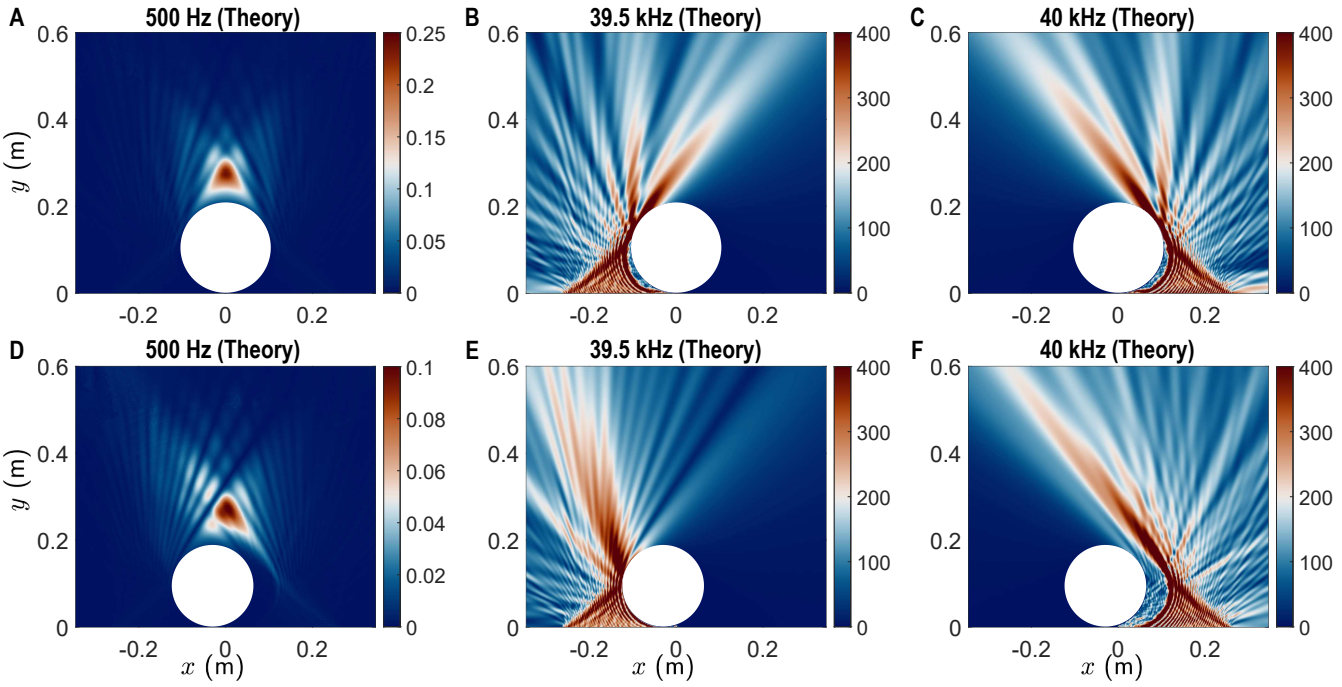

Fig. S17. Simulated sound field distributions with a larger source size of $a = 24\,\mathrm{cm}$. Other parameters defined in Fig. S11 are: $\Delta a = 25\,\mathrm{mm}$, $R_0 = 90\,\mathrm{mm}$, (A, B, C) $x_\mathrm{c} = 0, r_0 = 100\,\mathrm{mm}$, and (D, E, F) $x_\mathrm{c} = -30\,\mathrm{mm}, r_0 = 90\,\mathrm{mm}$. (A, D) Audio sound fields at 500 Hz. Self-bending ultrasonic beams at (B, E) 39.5 kHz and (C, F) 40 kHz.

Movie S1. Demonstration of the proposed audible enclave under a transient wideband audio signal excitation (a 9-second sample of music).